IEEE Photonics Journal
An IEEE Photonics Society Publication

Open Access

Enhanced Emission Efficiency of Deep Ultraviolet Light-Emitting AlGaN Multiple Quantum Wells Grown on an N-AlGaN Underlying Layer

Volume 8, Number 5, October 2016

Lei Li
Yuta Miyachi
Makoto Miyoshi
Takashi Egawa, ***Member, IEEE***

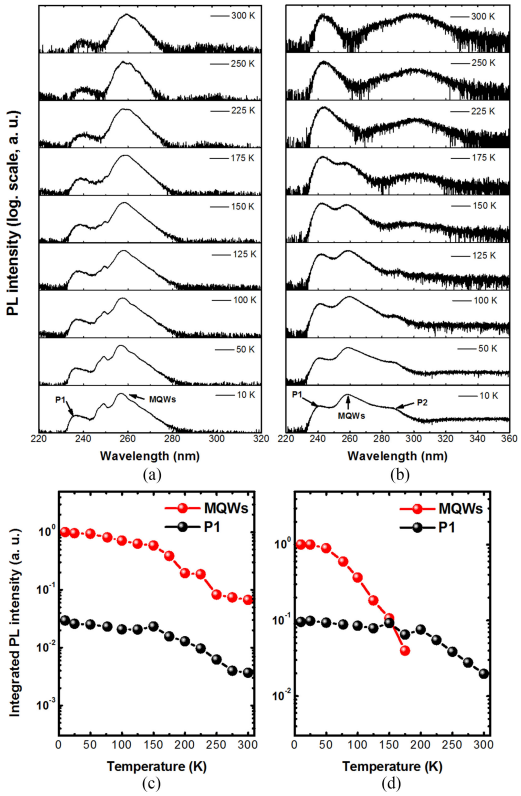

DOI: 10.1109/JPHOT.2016.2601439

Enhanced Emission Efficiency of Deep Ultraviolet Light-Emitting AlGaN Multiple Quantum Wells Grown on an N-AlGaN Underlying Layer

Lei Li, Yuta Miyachi, Makoto Miyoshi, and Takashi Egawa, *Member, IEEE*

Research Center for Nano Devices and Advanced Materials, Nagoya Institute of Technology, Nagoya 466-8555, Japan.

DOI:10.1109/JPHOT.2016.2601439

Manuscript received July 19, 2016; revised August 12, 2016; accepted August 15, 2016. Date of publication August 30, 2016; date of current version September 20, 2016. This work was supported in part by the Super Cluster Program of the Japan Science and Technology Agency (JST). Corresponding author: L. Li (e-mail: lilei443443@gmail.com)

Abstract: Remarkably enhanced light emission efficiency of AlGaN multiple quantum wells (MQWs) was realized by growing on an n-AlGaN underlying layer (UL). The parasitic peaks emitting from inactive regions can be effectively suppressed, and the nonradiative recombination process in AlGaN MQWs proved to be substantially lessened with the inclusion of the n-AlGaN UL. Numerical simulations showed that the electric field in AlGaN MQWs was reduced by 26%, which efficiently weakened the quantum-confined Stark effect (QCSE). Further analysis attributed this to the reduction of strain-induced piezoelectric electric field in the AlGaN well layer. The enhanced emission efficiency of AlGaN MQWs was therefore due to the greatly suppressed nonradiative recombination and reduced QCSE with the introduction of the n-AlGaN UL. The present research will be helpful to the future promotion of high-performance deep ultraviolet (DUV) optoelectronic devices, as well as to better understanding the recombination mechanism in AlGaN MQWs.

Index Terms: AlGaN multiple quantum wells (MQWs), n-AlGaN underlying layer (UL), quantum-confined Stark effect (QCSE), recombination process.

1. Introduction

Wurtzite $Al_xGa_{1-x}N$ alloys with a high AlN mole fraction (x) have attracted wide attention for optoelectronic applications in deep ultraviolet light-emitting diodes (DUV-LEDs) and lasers [1]–[12]. Towards the goal of commercial applications, the light emission efficiency of AlGaN multiple quantum wells (MQWs), which function as the core structure of DUV optoelectronic devices, has become one of the crucial issues. Unlike the InGaN MQWs, the light emission efficiency of AlGaN MQWs, especially its internal quantum efficiency (IQE), has been very sensitive to the crystal quality [13]–[15]. High dislocation density in AlGaN MQWs originating from the AlN buffer layer limits the value of IQE to date. On the other hand, the large internal electric field in the *c*-plane AlGaN MQWs leads to a significant charge carrier separation by quantum-confined Stark effect (QCSE) [16]–[20], which, in turn, results in small optical matrix elements and a low radiative recombination rate, and the light emission efficiency of AlGaN MQWs is consequently reduced.

Up to now, a number of studies focused on improving the crystal quality of AlN buffer layer have been done to boost the performance of AlGaN MQWs by special growth techniques [14], [21]–[25]. Although the electric field in AlGaN MQWs can be reduced via grown on nonpolar and semipolar AlN substrates [26], [27], the density of nonradiative recombination centers seems to be enhanced, which prevents their applications to efficient LEDs. Moreover, decreasing the well width can partly suppress the QCSE [28], but it is disadvantageous to overcome the efficiency droop effect in LEDs at high current injection. Cabalu *et al.* [29] reported that they succeeded in improving the light emission efficiency of AlGaN MQWs with markedly suppressed QCSE by the growth on textured GaN templates. Toropov *et al.* [30] reported a corrugated AlGaN MQW structure that exhibited an enhanced light emission realized by the change of growth mode to reduce the electric field. Apart from these, however, few achievements on the light emission efficiency enhancement of AlGaN MQWs by diminishing the electric field have been reported, especially on the structural design.

In the present study, we investigated the optical properties of AlGaN MQWs grown on an n-AlGaN UL, aiming to clarify the effect of the n-AlGaN UL on the light emission efficiency of the AlGaN MQWs. The optical properties of AlGaN MQWs grown on the n-AlGaN UL were fully discussed with those of comparative structures combined with numerical simulations.

2. Experimental Details

The AlGaN MQWs samples in this study were grown by metal organic chemical vapor deposition (MOCVD) system with a horizontal geometry reactor (Taiyo Nippon Sanso SR2000). A 500-nm-thick unintentionally doped $Al_{0.7}Ga_{0.3}N$ layer was initially deposited on a *c*-plane AlN/sapphire template (DOWA Electronics, typical linewidths: (002) $\sim$ 100-200 arcsec, (102) $\sim$ 1500-2000 arcsec), followed by a 1-μm-thick Si-doped $Al_{0.7}Ga_{0.3}N$ layer. Subsequently, a 20-nm-thick Si-doped $Al_{0.65}Ga_{0.35}N$ UL was grown, followed by three-period unintentionally doped $Al_{0.5}Ga_{0.5}N/Al_{0.6}Ga_{0.4}N$ (2 nm / 5 nm) MQWs. The Si concentration in these Si-doped layers was set to 8.4×10^{17} cm^{-3}. The threading dislocation density in the AlN/sapphire template (specially treated for epitaxy) and n-$Al_{0.7}Ga_{0.3}N$ layer was approximately 1.5×10^9 and 1.3×10^9 cm^{-2}, respectively, estimated from X-ray diffraction (XRD) measurement. For comparison, a similar AlGaN MQW structure without the n-AlGaN UL was grown.

For optical investigation, photoluminescence (PL) measurements were performed by using a frequency-quadrupled mode-locked Ti:sapphire laser ($\lambda = 210$ nm) as an excitation source, whose repetition rate and pulse width are 80 MHz and 100 fs, respectively. The time-resolved PL (TRPL) decay transients were acquired by a standard streak-camera system with a resolution of 15 ps through a single photon counting system combined with a photomultiplier tube. The average output excitation laser power was held constant at 7 mW. Samples were placed in a closed-cycle helium refrigerator during the temperature-dependent characterizations. XRD reciprocal space mapping (XRD-RSM) technique was carried out to study the strain distribution and its influence on the polarization field in the AlGaN MQWs for both samples. Besides, simulation study was conducted to investigate the band profile and electric field of AlGaN MQWs using a commercially available software SiLENSe [31].

3. Results and Discussion

The optical properties of these two samples were systematically compared by means of low temperature and temperature-dependent PL measurements. Fig. 1 shows the PL spectra taken at 10 K. A MQWs emission peak at $\lambda \sim$ 257 nm was observed in the sample with the n-AlGaN UL, which exhibited a slight 3 nm blueshift compared to the case without the n-AlGaN UL emitting at $\lambda \sim$ 260 nm. The integrated PL intensity of MQWs emission in the sample with the n-AlGaN UL was significantly improved, which was about 2.25 times that of the sample without the n-AlGaN UL, as obviously seen in Fig. 1. Meanwhile, the full width at half maximum of the PL spectrum of the sample with the n-AlGaN UL was 4.8 nm, which was reduced nearly by half with respect to the sample without the n-AlGaN UL, whose PL spectrum represented a FWHM of 9 nm. This denotes

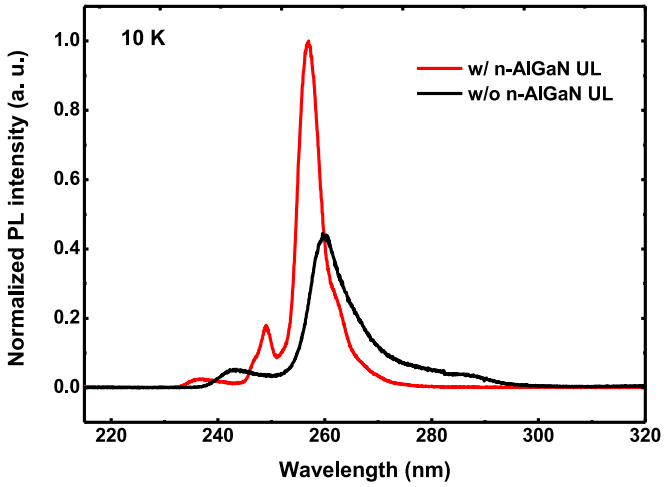

Fig. 1. PL spectra taken at 10 K, normalized to the peak of the sample with the n-AlGaN UL.

that the optical quality of the AlGaN MQWs was improved with the n-AlGaN UL. Notably, there was a peak emission close to $\lambda \sim 240$ nm for both samples, which was believed to be from the n-$Al_{0.7}Ga_{0.3}N$ layer [32]. Additionally, the emission peak at $\lambda \sim 248$ nm was considered to originate from the n-AlGaN UL.

The temperature-dependent PL spectra of the two samples in semi-logarithmic scale were shown in Fig. 2. Two typical light emission peaks, MQWs and P1, generated from the AlGaN MQWs and n-$Al_{0.7}Ga_{0.3}N$ layer, respectively, were distinguished for the sample with the n-AlGaN UL in Fig. 2(a). Correspondingly, the normalized integrated PL intensities of the peak emission from MQWs and P1 were shown in Fig. 2(c). The MQWs emission, which dominated in each PL spectrum under different temperatures, presented a gradually decrease on its integrated PL intensity. More specifically, the PL intensity ratio of MQWs to P1 was estimated from 34 at 10 K to 18 at 300 K. In contrast, diverse light emission behavior took place in the sample without the n-AlGaN UL in Fig. 2(b). The MQWs emission only exhibited in the range of 10-175 K, which indicated that more nonradiative recombination centers caused by threading dislocations or other crystal defects were activated in AlGaN MQWs with increasing the temperature, while the P1 peak was unquenched in the whole temperature range. Moreover, a deep-level emission at $\lambda \sim 287$ nm, marked by P2, was identified, and shifted to around 300 nm with a broad line shape, which probably resulted from Al vacancy and its complex in n-$Al_{0.7}Ga_{0.3}N$ layer [33], [34]. The PL intensity ratio of MQWs to P1 can be estimated from 10 at 10 K to 0.6 at 175 K, as shown in Fig. 2(d). Further, the integrated PL intensity of MQWs emission showed a drastic decrease above 50 K, and larger intensity of P1 peak than that in Fig. 2(c), was obviously seen. According to these results, it is deduced that the AlGaN MQW emission efficiency can be markedly enhanced by the introduction of the n-AlGaN UL, which suppressed the detrimental band edge luminescence from the layers beneath the AlGaN MQWs and light emission resulting from the defect-related deep levels in Si-doped AlGaN layers. The absence of the deep level luminescence from the n-AlGaN UL in Fig. 2(a) was likely to be due to the lower growth rate, which favors the point defects reduction during the MOCVD epitaxy, as well as the smaller thickness [35].

In order to determine the degree of carrier localization in AlGaN MQWs, we used the following two-channel Arrhenius equation to fit the normalized PL intensity, as demonstrated in Fig. 3:

$$I(T) = [1 + A\exp(-E_{A1}/k_BT) + B\exp(-E_{A2}/k_BT)]^{-1} \quad (1)$$

Here, $I(T)$ represents the normalized PL intensity as a function of $1/k_BT$, where k_B and T are the Boltzmann constant and absolute temperature, respectively. A and B are two parameters related

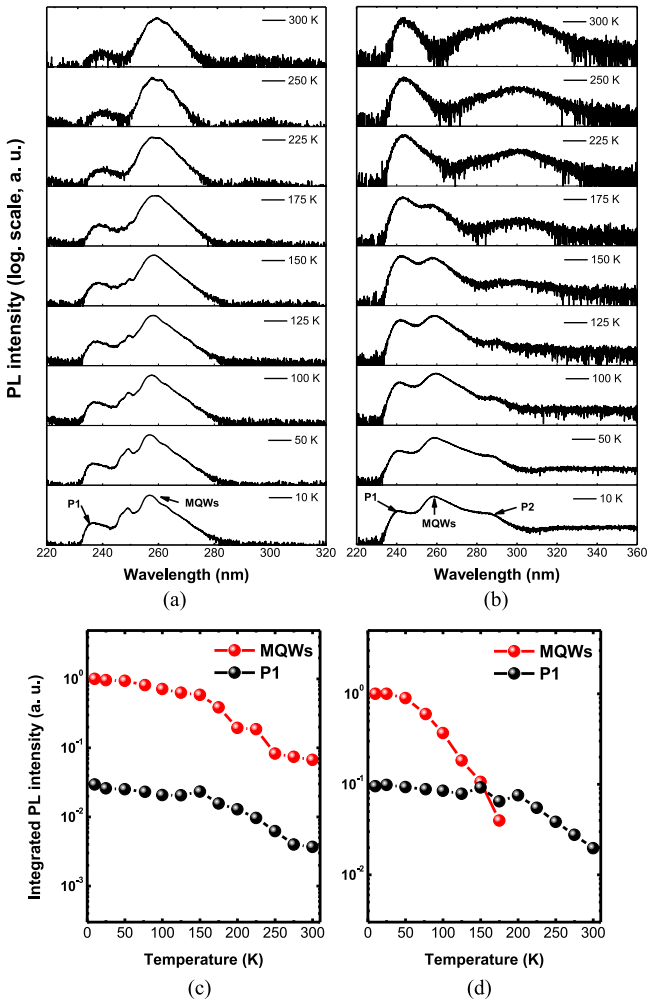

Fig. 2. Temperature-dependent PL results for samples (a) and (c) with the n-AlGaN UL and (b) and (d) without the n-AlGaN UL.

to the density of nonradiative recombination center in the samples. E_{A1} and E_{A2} are two activation energies, where E_{A1} is a potential barrier against the carriers hopping from shallow localized states to deeper ones, and E_{A2} is a potential barrier between the localized potential minima and the defect-related nonradiative recombination centers inside the MQWs [36], [37]. The parameters obtained from the fitted curves were summarized in Table 1. It was obvious that the density of nonradiative recombination center was greatly reduced in the sample with the n-AlGaN UL, which can improve the optical quality of the AlGaN MQWs shown in Fig. 1. The lower E_{A1} indicated that weaker exciton localization took place in the sample with the n-AlGaN UL at low temperature. Compared to the sample without the n-AlGaN UL, the activation energy E_{A2} was larger in the sample with the n-AlGaN UL, which means that carriers were prone to be localized in the potential minimum rather than reach the nonradiative recombination centers located inside the AlGaN MQWs at high temperature. As a result, a room-temperature IQE up to 6.7% of AlGaN MQWs, defined as the integrated PL intensity ratio between 300 and 10 K [$\eta_{\text{int}} = I_{\text{PL}}(300\,\text{K})/I_{\text{PL}}(10\,\text{K})$] [38], was achieved in the sample with the n-AlGaN UL. The inset of Fig. 3 shows the temperature-dependent peak energy variation of the AlGaN MQWs for the sample with the n-AlGaN UL. The peak energy exhibited a reversed "S-shaped" shift (increase – accelerated decrease – decelerated decrease) with increasing T. The initial blueshift of peak position was considered to be attributed to the

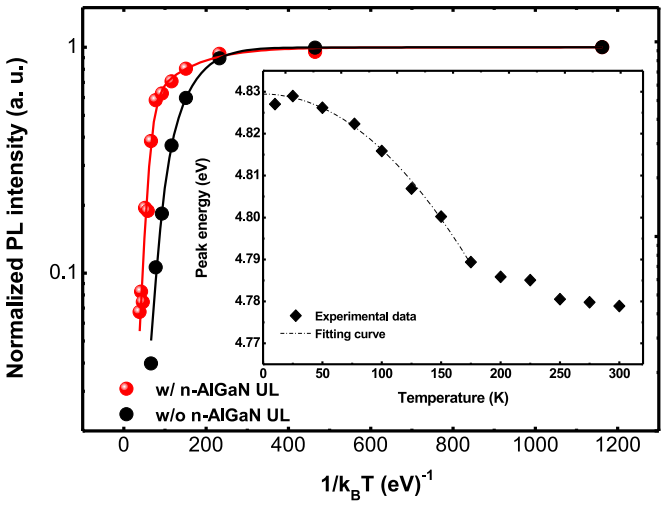

Fig. 3. Arrhenius plots of the normalized integrated PL intensity of the AlGaN MQWs for both samples. (Inset) Temperature-dependent peak energy of AlGaN MQWs for the sample with the n-AlGaN UL.

TABLE 1

Parameters Obtained by Fitting the Arrhenius Plot: *A* and *B* are Two Constants Related to the Density of Nonradiative Recombination Center, and E_{A1} and E_{A2} are Two Activation Energies

Type	*A*	*B*	E_{A1} (meV)	E_{A2} (meV)
w/ n-AlGaN UL	1.3	752.5	11.0	99.0
w/o n-AlGaN UL	14.7	1940.9	20.7	73.0

excitons repopulation from local potential minima to higher energy states due to the increased thermal energy up to 25 K. The subsequent temperature-dependent peak energy variation was found to well follow the Varshni equation [39], as fitted by the dashed line, which indicated that the accelerated redshift of peak energy varying from 25 to 175 K resulted from the temperature-induced bandgap shrinkage. The abnormal decelerated redshift of peak energy in the final part from 175 to 300 K was probably because the photon-generated carriers recombined before reaching the lower-energy tail states included in the AlGaN MQWs light emission, which extended the higher energy MQWs emission and weakened the temperature-dependent bandgap shrinkage [40].

To understand how the n-AlGaN UL influenced the recombination dynamics in AlGaN MQWs, temperature-dependent TRPL decay transients were conducted for both samples. Fig. 4(a) shows the low-temperature PL decay curves maintained at the peak emission energy. To measure the decay time, the non-linear PL decay curves were fitted by

$$I(t) = \exp\left(-\frac{t}{\tau_{PL}}\right) \tag{2}$$

where $I(t)$ is the normalized PL intensity at time t, and τ_{PL} is the effective PL lifetime. Here, τ_{PL} was defined as the time required for the PL intensity to decay by a factor of $1/e$ from its maximum [41], [42]. The radiative recombination lifetime τ_R and nonradiative recombination lifetime τ_{NR} can be derived from [41], [43]

$$\eta_{int}(T) = \frac{\tau_{PL}(T)}{\tau_R(T)}, \quad \frac{1}{\tau_{PL}(T)} = \frac{1}{\tau_R(T)} + \frac{1}{\tau_{NR}(T)} \tag{3}$$

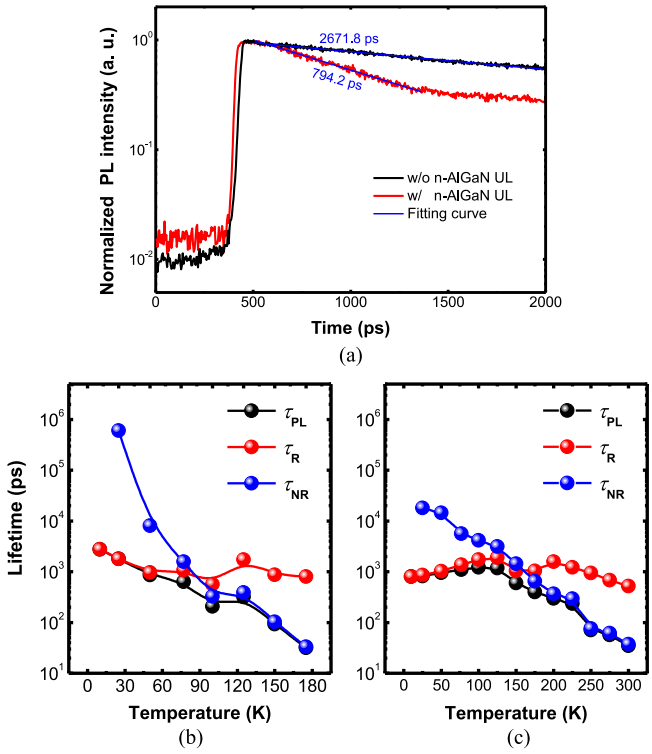

Fig. 4. (a) TRPL decay transients maintained at AlGaN MQWs peak emission for both samples at 10 K and temperature dependence of the measured τ_{PL} and calculated τ_R and τ_{NR} of AlGaN MQWs for sample (b) without and (c) with the n-AlGaN UL.

Based on the above, τ_{PL} was calculated to be 2671.8 and 794.2 ps for the sample without and with the n-AlGaN UL at 10 K, respectively, as shown in Fig. 4(a). This significant reduction of τ_{PL} led to the enhanced emission efficiency of the AlGaN MQWs grown on the n-AlGaN UL shown in Fig. 1. The τ_R of AlGaN MQWs for both samples was around 1000 ps in Fig. 4(b) and (c). Previous theoretical calculations have shown that τ_R of zero-dimensional (0D) exciton is almost independent of T [44], [45], and thus, it is understood that 0D exciton localization was formed in both samples. This may suggest that Al- and/or Ga-rich AlGaN localized structures exist in the AlGaN MQWs due to the Al-composition fluctuations, which needs further investigations to provide insight into understanding. Furthermore, the more fluctuant temperature-dependent variation of τ_R in the sample with the n-AlGaN UL reflected that the behaviors of other dimensional excitons cannot be excluded, and the effect of exciton localization in AlGaN MQWs was weaker than the case without the n-AlGaN UL, which was in good agreement with the results in Table 1. At the same time, τ_{NR} decreased rapidly at the initial stage with increasing T, and become dominant in the recombination lifetime from 100 K in the sample without the n-AlGaN UL. However, τ_{NR} in the sample with the n-AlGaN UL showed a gradual decrease with larger values in the whole temperature range and become dominant above 150 K. It was obvious that the nonradiative recombination process in AlGaN MQWs was sufficiently suppressed with the introduction of n-AlGaN UL, which can further improve the light emission.

In order to figure out the effect of the n-AlGaN UL on the AlGaN MQWs samples from the basic structural perspective, the conduction and valence band profiles of both structures were simulated by using the commercially available software SiLENSe. In this simulation, the ratio of the conduction and valence band offsets was assumed to be 7:3, and other parameters, such as piezoelectric and spontaneous polarization constants, were based on previous reports [7], [46]. Fig. 5 shows the

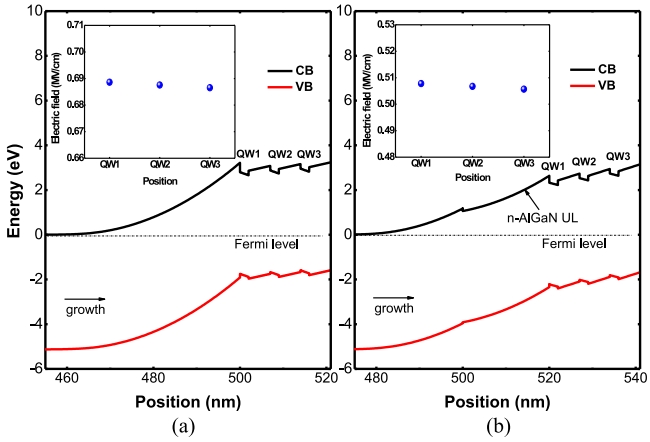

Fig. 5. Calculated conduction band (CB) and valence band (VB) profiles for sample (a) without and (b) with the n-AlGaN UL, where the Fermi level is located at 0 eV. (Insets) Calculated electric field in each QW.

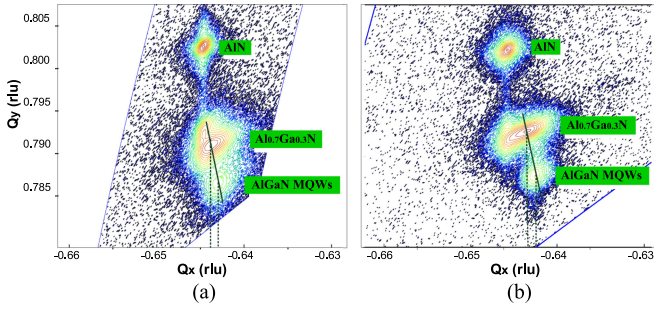

Fig. 6. XRD-RSMs around (114) reflection for samples (a) without and (b) with the n-AlGaN UL. The solid line represents the strain relaxation R(MQWs), and the dashed lines show the values of Q_x.

calculated band diagrams accompanied with the electric field of AlGaN MQWs for both samples. The built-in potential gradient across each QW of the samples without and with the n-AlGaN UL were calculated to be approximately 65 and 50 meV/nm, respectively. The reduction of built-in potential gradient represented that the n-AlGaN UL strongly modified the band bending between the n-$Al_{0.7}Ga_{0.3}N$ and AlGaN MQW layer. Simultaneously, the electric fields in AlGaN MQWs in the samples without and with the n-AlGaN UL were calculated to be 0.69 and 0.51 MV/cm, respectively, as seen in the insets of Fig. 5(a) and (b). The results showed that the electric field in the sample with the n-AlGaN UL was reduced by 26% compared with the case without the n-AlGaN UL. As is well known, the quantum-confined Stark effect (QCSE), which limits the emission efficiency of MQWs, can be suppressed by diminishing the electric field [47]–[49]. Therefore, we can conclude that the QCSE in AlGaN MQWs was weakened by introducing the n-AlGaN UL, which can further increase the radiative recombination rate, enlarge the peak energy of the MQWs light emission, and improve the light emission efficiency. The slight blueshift in peak energy of the AlGaN MQWs grown on the n-AlGaN UL at 10 K in Fig. 1 was, hence, attributed to this.

The electric field in the MQWs consists of contributions from the intrinsic spontaneous and strain-induced piezoelectric polarization fields [50]. The reduction of QCSE caused by the electric field was, hence, likely to be due to strain relaxation of the AlGaN MQWs grown on the n-AlGaN UL. To clarify the mechanism that caused the QCSE reduction by the n-AlGaN UL, XRD-RSM of the asymmetric (114) reflections were performed to investigate the strain distributions in these samples. Fig. 6 shows the measured (114) RSMs for the sample without and with the n-AlGaN UL. For the

hexagonal III-nitrides, the in-plane lattice constant a and out-of-plane lattice constant c can be obtained from the reciprocal coordinate Q_x and Q_y in the RSMs by [51]

$$a = \sqrt{\frac{4\left(h^2 + hk + k^2\right)}{3}}\frac{1}{Q_x},\ c = \frac{l}{Q_y}. \tag{4}$$

The degree of strain relaxation of AlGaN MQWs is defined as [52]

$$R(MQW_S) = \frac{a_{MQW_S} - a_{Al_{0.7}Ga_{0.3}N}}{a_{0\,MQW_S}(x) - a_{Al_{0.7}Ga_{0.3}N}} \tag{5}$$

where a_{MQWs} and a_{AlGaN} are measured lattice constants from RSMs, and a_{0MQWs} is the relaxed parameters predicted by Vegard's law. The Al content in the $Al_{0.7}Ga_{0.3}N$ layer was calculated to be approximately 70% $\pm$ 1% in both samples, which was in good agreement with the nominal design. It was found that the strain relaxation factor R(MQWs) was increased from 10.8% to 14.4% with the inclusion of the n-AlGaN UL. The relaxed AlGaN MQWs was compressively strained grown on n-$Al_{0.7}Ga_{0.3}N$ layer, and the increased strain relaxation factor indicated that the compressive strain of AlGaN MQWs became larger in the sample with the n-AlGaN UL than the case without it. More specifically, the strain status can be described in terms of the transformation between barrier and well within the AlGaN MQWs. The AlGaN barrier and well were compressive- and tensile-strained in the relaxed AlGaN MQWs in the sample without the n-AlGaN UL. With further strain relaxation, compressive strain in the AlGaN barrier was increased and tensile strain in the AlGaN well was released in the sample with the n-AlGaN UL. As the piezoelectric field P_{PZ} is closely related to the strain relaxation, the electric field variation in AlGaN QW can be estimated from P_{PZ} according to [53]

$$P_{PZ} = 2\left(e_{31} - e_{33}\frac{C_{13}}{C_{33}}\right)\varepsilon_{xx} \tag{6}$$

where e_{ij} and C_{ij} are the piezoelectric constants and elastic stiffness constants, respectively, linearly interpolated from AlN and GaN, and ε_{xx} is the in-plane strain of AlGaN QW. Based on the analysis above, the tensile strain ε_{xx} in AlGaN QW was released in the sample with the n-AlGaN UL, and consequently resulted in the reduction of P_{PZ}. The electric field was therefore weakened in AlGaN QW which caused the QCSE reduction with the introduction of the n-AlGaN UL. We can note that there is a diffraction peak locating between the AlN and the main $Al_{0.7}Ga_{0.3}N$ peak in Fig. 6(a), and it is nearly aligned with the AlN peak along Q_x vector. Therefore, it is considered that there was a thin AlGaN region pseudomorphically grown on the AlN/sapphire template in the sample without the n-AlGaN UL during epitaxy. This doesn't affect the comparison between the samples with and without the n-AlGaN UL.

4. Conclusion

In summary, we have investigated the optical properties of AlGaN MQWs structure grown on an n-AlGaN UL with comparative structures. Compared to the sample without the n-AlGaN UL, the integrated PL intensity of the AlGaN MQWs was increased by a factor of 2.25, and a much smaller FWHM of the PL spectrum was observed in the sample with the n-AlGaN UL at 10 K. Temperature-dependent PL measurements showed that the parasitic peaks emitting from inactive regions can be effectively suppressed by the n-AlGaN UL, which was beneficial for the light emission efficiency enhancement. Further analysis on the PL data indicated that the nonradiative recombination centers in AlGaN MQWs were greatly reduced, and carriers were prone to be localized in the potential minimum with the introduction of the n-AlGaN UL. TRPL measurements represented that 0D exciton localization took place in both samples; however, the nonradiative recombination process was evidently lessened with the introduction of the n-AlGaN UL. Band profile simulations showed that the inclusion of the n-AlGaN UL effectively modulated the band bending between the n-$Al_{0.7}Ga_{0.3}N$ and AlGaN MQW layer in terms of the decrease of the built-in potential gradient across each QW.

Simultaneously, the electric field in AlGaN MQWs was calculated to be 0.51 MV/cm in the sample with the n-AlGaN UL, which was reduced by 26% compared with the case without the n-AlGaN UL. XRD-RSMs attributed this to the reduction of strain-induced piezoelectric electric field in AlGaN well layer. The results showed that the QCSE in AlGaN MQWs was weakened in the sample with the n-AlGaN UL. The light emission efficiency of AlGaN MQWs was therefore enhanced due to the greatly suppressed nonradiative recombination and reduced QCSE with the introduction of the n-AlGaN UL. The present research has potential application for the DUV optoelectronic devices, as well as for better understanding the recombination mechanism in AlGaN MQWs.

Acknowledgment

One of the authors (Lei Li) would like to thank S. Kumagai for his technical assistance.

References

[1] J. P. Zhang *et al.*, "Milliwatt power deep ultraviolet light-emitting diodes over sapphire with emission at 278 nm," *Appl. Phys. Lett.*, vol. 81, no. 26, pp. 4910–4912, 2002.
[2] Y. Taniyasu, M. Kasu, and T. Makimoto, "An aluminium nitride light-emitting diode with a wavelength of 210 nanometres," *Nature*, vol. 441, no. 7091, pp. 325–328, 2006.
[3] H. Hirayama, Y. Tsukada, T. Maeda, and N. Kamata, "Marked enhancement in the efficiency of deep-ultraviolet AlGaN light-emitting diodes by using a multiquantum-barrier electron blocking layer," *Appl. Phys. Exp.*, vol. 3, 2010, Art. no. 031002.
[4] C. Pernot *et al.*, "Improved efficiency of 255–280 nm AlGaN-based light-emitting diodes," *Appl. Phys. Exp.*, vol. 3, 2010, Art. no. 061004.
[5] M. Shatalov *et al.*, "AlGaN deep-ultraviolet light-emitting diodes with external quantum efficiency above 10%," *Appl. Phys. Exp.*, vol. 5, 2012, Art. no. 082101.
[6] J. R. Grandusky *et al.*, "270 nm pseudomorphic ultraviolet light-emitting diodes with over 60 mW continuous wave output power," *Appl. Phys. Exp.*, vol. 6, 2013, Art. no. 032101.
[7] F. Mehnke *et al.*, "Efficient charge carrier injection into sub-250 nm AlGaN multiple quantum well light emitting diodes," *Appl. Phys. Lett.*, vol. 105, 2014, Art. no. 051113.
[8] S. Inoue, T. Naoki, T. Kinoshita, T. Obata, and H. Yanagi, "Light extraction enhancement of 265 nm deep-ultraviolet light-emitting diodes with over 90 mW output power via an AlN hybrid nanostructure," *Appl. Phys. Lett.*, vol. 106, 2015, Art. no.131104.
[9] X. L. Ji *et al.*, "Tailoring of energy band in electron-blocking structure enhancing the efficiency of AlGaN-based deep ultraviolet light-emitting diodes," *IEEE Photon. J.*, vol. 8, 2016, Art. no. 1600607.
[10] J. Zhang and N. Tansu, "Engineering of AlGaN-delta-GaN quantum-well gain media for mid- and deep-ultraviolet lasers," *IEEE Photon. J.*, vol. 5, 2013, Art. no. 2600209.
[11] X. H. Li *et al.*, "Low-threshold stimulated emission at 249 nm and 256 nm from AlGaN-based multiple-quantum-well lasers grown on sapphire substrates," *Appl. Phys. Lett.*, vol. 105, 2014, Art. no. 141106.
[12] X. H. Li *et al.*, "Demonstration of transverse-magnetic deep-ultraviolet stimulated emission from AlGaN multiple-quantum-well lasers grown on a sapphire substrate," *Appl. Phys. Lett.*, vol. 106, 2015, Art. no. 041115.
[13] M. Kneissl *et al.*, "Advances in group III-nitride-based deep UV light-emitting diode technology," *Semicond. Sci. Technol.*, vol. 26, 2011, Art. no. 014036.
[14] K. Ban *et al.*, "Internal quantum efficiency of whole-composition-range AlGaN multiquantum wells," *Appl. Phys. Exp.*, vol. 4, 2011, Art. no. 052101.
[15] M. Miyoshi, M. Kato, and T. Egawa, "Internal quantum efficiency of whole-composition-range AlGaN multiquantum wells," *Semicond. Sci. Technol.*, vol. 29, 2014, Art. no. 075024.
[16] T. Takeuchi *et al.*, "Quantum-confined stark effect due to piezoelectric fields in GaInN strained quantum wells," *Jpn. J. Appl. Phys.*, vol. 36, no. 4A, pp. L382–L385, 1997.
[17] J. S. Im, H. Kollmer, J. Off, A. Sohmer, F. Scholz, and A. Hangleiter, "Reduction of oscillator strength due to piezoelectric fields in GaN/AlxGa1-xN quantum wells," *Phys. Rev. B,* vol. 57, no. 16, pp. R9435–R9438, 1998.
[18] T. Deguchi *et al.*, "Quantum-confined stark effect in an AlGaN/GaN/AlGaN single quantum well structure," *Jpn. J. Appl. Phys.*, vol. 38, no. 8B, pp. L914–L916, 1999.
[19] S. F. Chichibu *et al.*, "Impact of internal electric field and localization effect on quantum well excitons in AlGaN/GaN/InGaN light emitting diodes," *Phys. Status Solidi (A)*, vol. 183, no. 1, pp. 91–98, 2001.
[20] C. Y. Chen, Y. C. Lu, D. M. Yeh, and C. C. Yang, "Influence of the quantum-confined stark effect in an InGaN/GaN quantum well on its coupling with surface plasmon for light emission enhancement," *Appl. Phys. Lett.*, vol. 90, 2007, Art. no. 183114.
[21] T. Koida *et al.*, "Improved quantum efficiency in nonpolar (11-20) AlGaN/GaN quantum wells grown on GaN prepared by lateral epitaxial overgrowth," *Appl. Phys. Lett.*, vol. 84, no. 19, pp. 3768–3770, 2004.
[22] H. Hirayama *et al.*, "222–282 nm AlGaN and InAlGaN-based deep-UV LEDs fabricated on high-quality AlN on sapphire," *Phys. Status Solidi (A)*, vol. 206, no. 6, pp. 1176–1182, 2009.
[23] J. Wu, K. Okuura, H. Miyake, and K. Hiramatsu, "Effects of substrate plane on the growth of high quality AlN by hydride vapor phase epitaxy," *Appl. Phys. Exp.*, vol. 2, 2009, Art. no. 111004.

[24] R. G. Banal, M. Funato, and Y. Kawakami, "Extremely high internal quantum efficiencies from AlGaN/AlN quantum wells emitting in the deep ultraviolet spectral region," *Appl. Phys. Lett.*, vol. 99, 2011, Art. no. 011902.
[25] Z. Bryan, I. Bryan, J. Xie, S. Mita, Z. Sitar, and R. Collazo, "High internal quantum efficiency in AlGaN multiple quantum wells grown on bulk AlN substrates," *Appl. Phys. Lett.*, vol. 106, 2015, Art. no. 142107.
[26] T. J. Badcock *et al.*, "Optical properties of GaN/AlGaN quantum wells grown on nonpolar substrates," *Appl. Phys. Lett.*, vol. 93, 2008, Art. no. 101901.
[27] M. Leroux *et al.*, "Stark effect in ensembles of polar (0001) Al0.5Ga0.5N/GaN quantum dots and comparison with semipolar (11−22) ones," *J. Appl. Phys.*, vol. 116, 2014, Art. no. 034308.
[28] R. Butte and N. Grandjean, *Effects of Polarization in Optoelectronic Quantum Structures, Polarization Effects in Semiconductors*. New York, NY, USA: Springer, 2008.
[29] J. S. Cabalu, C. Thomides, T. D. Moustakas, S. Riyopoulos, L. Zhou, and D. J. Smith, "Enhanced internal quantum efficiency andlight extraction efficiency from textured GaN/AlGaN quantum wells grown by molecular beam epitaxy," *J. Appl. Phys.*, vol. 99, 2006, Art. no. 064904.
[30] A. A. Toropov *et al.*, "Suppression of the quantum-confined Stark effect in AlxGa1−xN/AlyGa1−yN corrugated quantum wells," *J. Appl. Phys.*, vol. 114, 2013, Art. no. 124306.
[31] STR Group, Ltd., *Simulations are based on the software package SiLENSe 5.4*, Portsmouth, U.K.: STR.
[32] A. Bhattacharyya, T. D. Moustakas, L. Zhou, D. J. Smith, and W. Hug, "Deep ultraviolet emitting AlGaN quantum wells with high internal quantum efficiency," *Appl. Phys. Lett.*, vol. 94, 2009, Art. no. 181907.
[33] N. Nepal, M. L. Nakarmi, J. Y. Lin, and H. X. Jiang, "Photoluminescence studies of impurity transitions in AlGaN alloys," *Appl. Phys. Lett.*, vol. 89, 2006, Art. no. 092107.
[34] C. Stampfl and C. G. Van de Walle, "Theoretical investigation of native defects, impurities, and complexes in aluminum nitride," *Phys. Rev. B*, vol. 65, 2002, Art. no. 155212.
[35] P. Gibart, "Metal organic vapour phase epitaxy of GaN and lateral overgrowth," *Rep. Progress Phys.*, vol. 67, no. 5, pp. 667–715, 2004.
[36] J. S. Hwang *et al.*, "Direct comparison of optical characteristics of InGaN-based laser diode structures grown on pendeo epitaxial GaN and sapphire substrates," *Appl. Phys. Lett.*, vol. 90, 2007, Art. no. 131908.
[37] J. Bai, Q. Wang, T. Wang, A. G. Cullis, and P. J. Parbrook, "Optical and microstructural study of a single layer of InGaN quantum dots," *J. Appl. Phys.*, vol. 105, 2009, Art. no. 053505.
[38] V. Ramesh, A. Kikuchi, K. Kishino, M. Funato, and Y. Kawakami, "Strain relaxation effect by nanotexturing InGaN/GaN multiple quantum well," *J. Appl. Phys.*, vol. 107, 2010, Art. no. 114303.
[39] Y. P. Varshni, "Temperature dependence of the energy gap in semiconductors," *Physica*, vol. 34, no. 1, pp. 149–154, 1967.
[40] J. P. Zeng *et al.*, "Temperature-dependent emission shift and carrier dynamics in deep ultraviolet AlGaN/AlGaN quantum wells," *Phys. Status Solidi (RRL)*, vol. 7, no. 4, pp. 297–300, 2013.
[41] S. F. Chichibu *et al.*, "Origin of defect-insensitive emission probability in In-containing (Al,In,Ga)N alloy semiconductors," *Nature Mater.*, vol. 5, no. 10, pp. 810–816, 2006.
[42] M. J. Davies *et al.*, "A comparison of the optical properties of InGaN/GaN multiple quantum well structures grown with and without Si-doped InGaN prelayers," *J. Appl. Phys.*, vol. 119, 2016, Art. no. 055708.
[43] S. F. Chichibu, K. Hazu, T. Onuma, and A. Uedono, "Collateral evidence for an excellent radiative performance of Al x Ga1− x N alloy films of high AlN mole fractions," *Appl. Phys. Lett.*, vol. 99, 2011, Art. no. 051902.
[44] H. Gotoh, H. Ando, T. Takagahara, H. Kamada, A. C. Pirson, and J. Temmyo, "Effects of dimensionality on radiative recombination lifetime of excitons in thin quantum boxes of intermediate regime between zero and two dimensions," *Jpn. J. Appl. Phys.*, vol. 36, no. 6B, pp. 4204–4208, 1997.
[45] L. Marsal *et al.*, "Zero-dimensional excitons in CdTe/ZnTe nanostructures," *J. Appl. Phys.*, vol. 91, no. 8, pp. 91–98, 2002.
[46] L. Li, T. Tsutsumi, Y. Miyachi, M. Miyoshi, and T. Egawa, "Improved performance of AlGaN-based deep ultraviolet light-emitting diodes with n-AlGaN underlayers," *Semicond. Sci. Technol.*, vol. 30, 2015, Art. no. 125012.
[47] C. Roberts, Q. Yan, M.-S. Miao, and C. G. Van de Walle, "Confinement effects on valence-subband character and polarization anisotropy in (11-22) semipolar InGaN/GaN quantum wells," *J. Appl. Phys.*, vol. 111, 2012, Art. no. 073113.
[48] C. Huang *et al.*, "Enhanced efficiency and reduced spectral shift of green light-emitting-diode epitaxial structure with prestrained growth," *J. Appl. Phys.*, vol. 104, 2008, Art. no. 123106.
[49] T. Akasaka, H. Gotoh, Y. Kobayashi, H. Nakano, and T. Makimoto, "InGaN quantum wells with small potential fluctuation grown on InGaN underlying layers," *Appl. Phys. Lett.*, vol. 89, 2006, Art. no. 101110.
[50] T. Takeuchi *et al.*, "Determination of piezoelectric fields in strained GaInN quantum wells using the quantum-confined Stark effect," *Appl. Phys. Lett.*, vol. 73, no. 12, pp. 1691–1693, 1998.
[51] M. A. Moram and M. E. Vickers, "X-ray diffraction of III-nitrides," *Rep. Prog. Phys.*, vol. 72, 2009, Art. no. 036502.
[52] S. Pereira *et al.*, "Strain and composition distributions in wurtzite InGaN/GaN layers extracted from x-ray reciprocal space mapping," *Appl. Phys. Lett.*, vol. 80, no. 21, pp. 3913–3915, 2002.
[53] O. Ambacher *et al.*, "Two-dimensional electron gases induced by spontaneous and piezoelectric polarization charges in N- and Ga-face AlGaN/GaN heterostructures," *J. Appl. Phys.*, vol. 85, no. 6, pp. 3222–3233, 1999.